

Uncertainty Analysis of the Absorbed Dose to Regions of the Lung per Unit Exposure to Radon Progeny in a Mine

J W Marsh and A Birchall

ABSTRACT

The European Union project Alpha-Risk aims to quantify the cancer and non-cancer risks associated with multiple chronic radiation exposures by epidemiological studies, organ dose calculation and risk assessment. In the framework of this project, absorbed doses to regions of the lung of individual miners have been calculated. The relatively large dose to the lung mainly arises from the exposure to radon progeny. A parameter uncertainty analysis has been performed to derive the frequency distribution of the absorbed doses to regions of the lung per unit exposure to radon progeny. The analysis was performed using the ICRP Publication 66 Human Respiratory Tract Model (HRTM). It is assumed that the HRTM is a realistic representation of the physical and biological processes, and that the parameter values are uncertain. The parameter probability distributions used in the analysis were based upon measurement data published in the open literature. Parameters considered include: (i) aerosol parameters, (ii) subject related parameters such as breathing rate and fraction breathed through nose, (iii) target cell parameters such as depth of basal and secretory cell layer, and (iv) the absorption rates of radon progeny. Calculations were performed for two exposure scenarios: (i) wet drilling + medium ventilation, and (ii) wet drilling + good ventilation + diesel engines. Parameters characterising the frequency distributions of the absorbed doses are presented.

This study was partially funded by the European contract Alpha-Risk (FP6-516483).

© Health Protection Agency
Centre for Radiation, Chemical and Environmental Hazards
Radiation Protection Division
Chilton, Didcot, Oxfordshire OX11 0RQ

Approval: April 2009
Publication: May 2009
£15.00
ISBN 978-0-85951-642-6

This report from HPA Radiation Protection Division reflects understanding and evaluation of the current scientific evidence as presented and referenced in this document.

CONTENTS

1	Introduction	1
2	Method of analysis	2
3	Assignment of probability distributions for parameters	2
	3.1 Aerosol parameters	4
	3.1.1 Exposure conditions: Wet drilling + medium ventilation + no diesel engines	4
	3.1.2 Exposure conditions: Wet drilling + good ventilation + diesel engines	6
	3.2 Subject related parameters	7
	3.2.1 Breathing rate	8
	3.2.2 Fraction breathed through nose	10
	3.3 Target cell parameters	11
	3.4 Absorption parameters	12
	3.4.1 Unattached radon progeny	12
	3.4.2 Attached radon progeny	13
4	Classification of errors	15
5	Results	17
	5.1 Exposure conditions: Wet drilling + medium ventilation	17
	5.2 Exposure conditions: Wet drilling + good ventilation + diesel engines	21
6	Discussion	22
7	Conclusion	24
8	Acknowledgements	24
9	References	25

1 INTRODUCTION

The European Union project Alpha-Risk aims to quantify the cancer and non-cancer risks associated with multiple chronic radiation exposures by epidemiological studies, organ dose calculation and risk assessment. It pools major epidemiological studies in Europe including the German, French and Czech uranium miner studies. As part of this project the annual absorbed doses to regions of the lung, red bone marrow, liver and kidney of each individual miner within the cohorts needs to be assessed.

An important source of exposure in the mines is the exposure to radon progeny which mainly accounts for the dominant dose to the lung. A large proportion of the inhaled radon progeny deposits in the respiratory airways of the lung and because of their relatively short half lives (less than half an hour) the radon progeny will decay mainly in the lung before being cleared either by absorption into blood or by particle transport to the alimentary tract. Two of the short-lived radon progeny (^{218}Po , ^{214}Po) decay by alpha emission and it is the energy from these alpha particles that accounts for the dominant dose to the lung.

The historical unit of exposure to radon progeny used in the uranium mining environment is the working level month (WLM) which is related to the potential alpha energy concentration (PAEC) of its short lived progeny (ICRP 1990). Thus the absorbed doses are expressed in terms of mGy per WLM.

The ICRP Publication 66 Human Respiratory Tract Model (ICRP 1994) (HRTM) has been used to calculate the absorbed doses to the following regions of the lung:

- BB_{bas} , the basal cell layer of the bronchial region (BB). The BB region consists of the trachea and airway generations 1-8.
- BB_{sec} , the secretory cell layer of BB region.
- bb , the bronchiolar region that consists of the bronchioles, terminal bronchioles and the respiratory bronchioles (airway generations 9 -18). The target cells in the bb region are the clara cells, which is a type of secretory cell.
- Al , the alveolar-interstitial region (i.e. the gas exchange region).

The uncertainty of the calculated absorbed doses to regions of the lung needs to be assessed. To do this a parameter uncertainty analysis has been performed on the HRTM to derive the frequency distribution of the absorbed doses per WLM for an individual miner. It is assumed that the HRTM is a realistic representation of the physical and biological processes, and that the parameter values are uncertain. Thus, the effects of different morphometric lung models on the deposition were not considered.

In a parameter uncertainty analysis all the parameter values are varied simultaneously according to their hypothesised probability distributions, and

correlations between parameters are taken into account. In this way a frequency distribution of the doses can be produced.

The probability distributions for the parameter values were chosen in order to represent variations in exposure conditions in a mine and due to variations among individual miners.

For the purposes of dose calculation miners were classified into different categories that define the exposure scenarios and the levels of physical activity (Marsh *et al*, 2008). In this uncertainty analysis two types of exposure scenarios were considered:

- Wet drilling + medium ventilation
- Wet drilling + good ventilation + diesel engines

Diesel engines were first used in the French and German mines during the 1970s. For mines with diesel engines operating, the diesel aerosol dominates the mine aerosol and therefore this needs to be considered when calculating doses to miners.

This document describes the methodology and presents the results of the uncertainty analysis.

2 METHOD OF ANALYSIS

The HPA computer program RADEP (Radon Dose Evaluation Program) (Marsh and Birchall, 2000), which implements the HRTM to calculate the absorbed dose to regions of the lung, was optimised for use in the uncertainty analysis. The parameter uncertainty analysis was carried out by performing a Monte Carlo simulation, in which each of the parameter values is chosen randomly from its hypothesised probability distributions. Correlations between parameters were taken into account. For each run, the absorbed dose was computed producing a frequency distribution of doses. As the calculations are time consuming, the sampling process was optimised according to the Latin Hypercube method (Iman and Conover, 1982).

3 ASSIGNMENT OF PROBABILITY DISTRIBUTIONS FOR PARAMETERS

The parameters considered include (i) aerosol parameters, (ii) subject related parameters such as breathing rate and fraction breathed through nose, (iii) target cell parameters such as depth of target cell layer, and (iv) the absorption rates of radon progeny.

The probability distributions assigned to each of the parameters are given in Tables 1 – 4. Four types of probability distributions (Figure 1) were used to

represent the uncertainty in the parameter values, and these distributions are defined in terms of parameters 'a' and 'b':

Rectangular distribution

Uniform probability density function (pdf) between 'a' and 'b' and zero for values outside this range.

Right-angled triangular distribution (positive gradient)

The pdf is zero for values of 'x' less than 'a' and greater than 'b'. For values of 'x' between a and 'b' (i.e. $a < x < b$) the pdf equals $2(x-a)/(b-a)^2$, thus the mode is at 'b'.

Normal distribution

The mean is given by the value 'a' and the standard deviation is given by 'b'.

Lognormal distribution

The median is given by the value 'a' and the geometric standard deviation is given by 'b'.

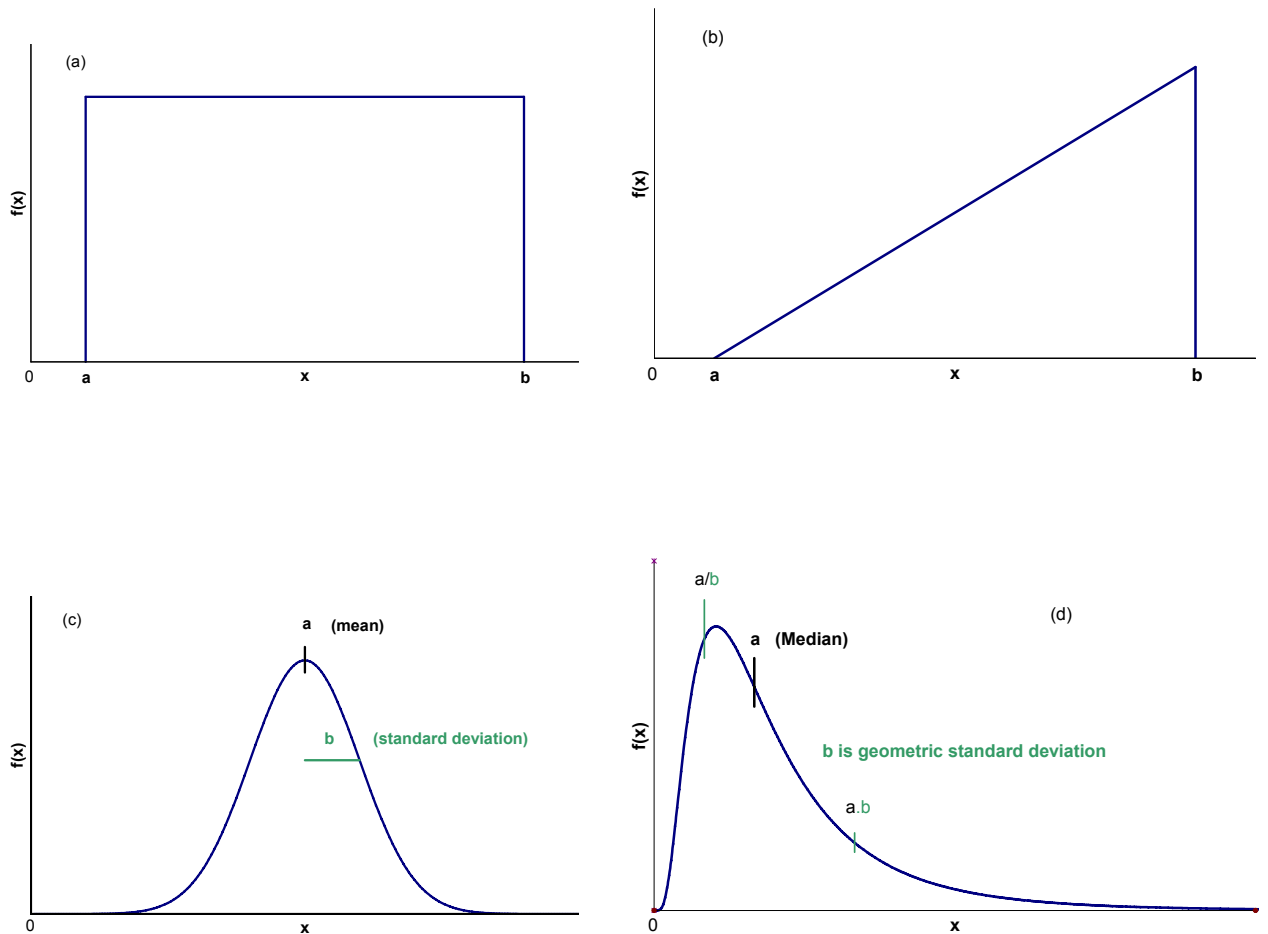


Figure 1 Probability distributions used to represent the uncertainty in the parameter values: (a) rectangular distribution, (b) triangular distribution (positive gradient), (c) normal distribution and (d) lognormal distribution. For the lognormal distribution there is a probability of about 68% that the value lies between a/b and ab .

The assignment of the parameter probability distributions were based upon measured data published in the open literature. However, in most cases subjective judgements had to be made. For example, when there had only been a few measurements of the parameter in question or when it was only known to lie between two values, a rectangular distribution was assumed.

3.1 Aerosol parameters

The radon progeny aerosol in the atmosphere is created in two steps. After decay of the radon gas, the freshly formed radionuclides (^{218}Po , ^{214}Pb , ^{214}Bi) react rapidly (< 1 s) with trace gases and vapours and grow by cluster formation to form particles around 1 nm. These are referred to as unattached particles. The unattached particles may also attach to existing aerosol particles in the atmosphere within 1 – 100 s forming the so-called attached particles. Typically, the activity size distribution of the attached particles in a mine can be described by a lognormal distribution with an activity median aerodynamic diameter (AMAD) between about 130 nm and 350 nm (Butterweck *et al* 1992).

The assignment of the parameter probability distributions for the aerosol parameters were mainly based on the measurements in mines performed by Butterweck *et al* (1992), Porstendörfer and Reineking (1999) and Bigu (1990), and on the values recommended by Birchall and James (1994). Aerosol parameter values were considered for two exposure scenarios:

- Wet drilling + medium ventilation
- Wet drilling + good ventilation + diesel engines

3.1.1 Exposure conditions: Wet drilling + medium ventilation + no diesel engines

Table 1 gives the parameter probability distributions for aerosol parameters that are appropriate for a mine with medium ventilation, wet drilling and with no diesel engines.

The magnitude of the unattached fraction primarily depends on the concentration of particles of ambient aerosol. Typically for a mine the number particle concentration is high so the unattached fraction is low; less than 3% of the total PAEC.

The relative activity size distribution of unattached radon progeny cluster depends on the concentration of water vapour, trace gases and the electrical charge distribution of the radionuclides in the atmospheric air. Porstendörfer (2001) found that under 'normal' conditions concerning humidity and radon concentration the activity size distribution of the unattached progeny can be approximated with three lognormal distributions. The activity median thermodynamic diameter (AMTD) values measured were 0.6 nm, 0.85 nm, and 1.3 nm with geometric standard deviations (σ_g) of about 1.2. In places with high radon concentration and/or high humidity the fraction with the greatest AMTD value (1.3 nm) was not registered. For simplicity, a uniform distribution for the

AMTD of the unattached radon progeny was assumed ranging from 0.5 – 1.3 nm (Table 1).

The size of the unattached progeny is assumed to remain constant in the lung. However, some of the ambient aerosols are unstable in saturated air (i.e. hygroscopic) and are assumed to grow instantaneously on inhalation by a given factor. Sinclair *et al* (1974) found that atmospheric particles in their laboratory increased in diameter by a factor of 2 or more when the relative humidity increased from zero to 98%. Because the relative humidity is high in a mine and the mine aerosol is likely to be less hygroscopic, the hygroscopic growth factor is likely to be less than 2. A uniform distribution was therefore assumed for the hygroscopic growth factor ranging from 1 to 2 (Table 1). For modeling purposes, it is assumed that the thermodynamic diameter increases instantaneously by the hygroscopic growth factor as the particle enters the nose or mouth. As a result the density will also change. For example, assuming a hygroscopic growth factor of 1.5 and an initial density of 1.4 g cm^{-3} will result in the density being reduced to 1.12 g cm^{-3} .

Table 1 Representative values and probability distributions of aerosol parameters for a mine with medium ventilation, wet drilling and with no diesel engines.

Description of parameter	Representative value	Probability distribution		
		Form	A	B
Unattached fraction ^a	0.01	Lognormal	0.008	2.0
Unattached aerosol size (AMTD) ^b	0.8 nm	Rectangular	0.5 nm	1.3 nm
Unattached dispersion	1.3	Rectangular	1.1	1.4
Unattached hygroscopic growth factor	1.0	Fixed		
Unattached particle density	1 g cm^{-3}	Fixed		
Unattached shape factor	1	Fixed		
Attached fraction	0.99			
Attached aerosol size (AMAD) ^c	250 nm	Rectangular	150 nm	350 nm
Attached dispersion	2.2	Rectangular	1.5	3.5
Attached hygroscopic growth factor	1.5	Rectangular	1.0	2.0
Attached particle density	1.4 g cm^{-3}	Rectangular $1+(2 \mathbf{R1})^d$	1 g cm^{-3}	3 g cm^{-3}
Attached shape factor	1.1	$1+(0.9 \mathbf{R1})^d$	1	1.9
Equilibrium factor	0.4	Rectangular	0.1	0.6

- (a) Expressed as a fraction of total potential alpha energy concentration (PAEC) of the radon progeny mixture. The 95% confidence interval is 0.002 -0.03.
- (b) AMTD is the activity median thermodynamic diameter of the aerosol.
- (c) AMAD is the activity median aerodynamic diameter of the aerosol.
- (d) Random variable **R1** has a uniform probability distribution between 0 and 1, and is used to introduce a correlation between the density and the shape factor

It was assumed that the attached particle density and the attached particle shape factor are correlated Birchall and James (1994). This is reasonable because for radon progeny attached to water droplets both the density and the shape factor will tend to unity. Measurements of the density of mine dust gave

a range of 2.4 to 2.7 g cm⁻³ indicating silica as the primary component (Harley, 2007). For a mine without diesel engines, a uniform distribution for the density of the attached radon progeny particle was therefore assumed ranging from 1 to 3 g cm⁻³ (Table 1).

3.1.2 Exposure conditions: Wet drilling + good ventilation + diesel engines

Table 2 gives the parameter probability distributions for aerosol parameters that are appropriate for a mine with good ventilation, wet drilling and with diesel engines operating.

Generally, for mines with diesel engines operating, the diesel aerosol dominates the mine aerosol resulting in a very low unattached fraction and an AMAD of 200 nm for the attached progeny (Butterweck *et al* 1992, Porstendörfer and Reineking 1999) (Table 2). Diesel aerosols are hydrophobic (Cavallo 2000, Weingartner *et al* 1997), so the attached hygroscopic growth factor was fixed at 1.0.

Table 2 Representative values and probability distributions of aerosol parameters for a mine with good ventilation, wet drilling and with diesel engines.

Description of parameter	Representative value	Probability distribution		
		Form	A	B
Unattached fraction ^a	0.006	Lognormal	0.005	2.0
Unattached aerosol size (AMTD) ^b	0.8 nm	Rectangular	0.5 nm	1.3 nm
Unattached dispersion	1.3	Rectangular	1.1	1.4
Unattached hygroscopic growth factor	1.0	Fixed		
Unattached particle density	1 g cm ⁻³	Fixed		
Unattached shape factor	1	Fixed		
Attached fraction	0.994			
Attached aerosol size (AMAD) ^c	200 nm	Lognormal	220 nm	1.3
Attached dispersion	2.0	Rectangular	1.5	3.0
Attached hygroscopic growth factor	1.0	Fixed		
Attached particle: effective density ^d	(e)	(e)		
Equilibrium factor	0.4	Rectangular	0.1	0.5

(a) Expressed as a fraction of total potential alpha energy concentration (PAEC) of the radon progeny mixture. The 95% confidence interval is 0.002 -0.03.

(b) AMTD is the activity median thermodynamic diameter of the aerosol.

(c) AMAD is the activity median aerodynamic diameter of the aerosol.

(d) Effective density is the ratio of the particle density to the shape factor (Park *et al* 2003).

(e) The effective density is determined from the given thermodynamic diameter of the particle (Equation 1, Figure).

Several workers have calculated the effective density of diesel exhaust particles from measurements of the thermodynamic and aerodynamic diameters of the exhaust particles (Park *et al* 2003). The effective density is the ratio of the particle density to the shape factor. Park *et al* (2003) measured the thermodynamic diameter (d_{th}) and the mass of diesel exhaust particles to

determine the effective density (ρ_{eff}). Figure 2 shows the results of their measurements for diesel exhaust particles from a John Deere 4045, 4 cylinder, 4.5 litre engine operating with 3 different loads. Results indicated that ρ_{eff} decreases with increasing d_{th} in the size range from 50 – 300 nm (Figure 2). This mainly occurs because particles become more highly agglomerated as size increases. The smaller particles are more compact than the larger particles and therefore have a higher effective density.

The following equation was fitted to the data of Park *et al* (2003):

$$\rho_{\text{eff}} = 2.70 - 0.42 \log_e(d_{\text{th}}) \quad \text{if } 50 \text{ nm} < d_{\text{th}} < 300 \text{ nm} \quad (1)$$

Where ρ_{eff} is measured in g cm^{-3} and d_{th} is measured in nm. The above correlation between ρ_{eff} and d_{th} was assumed in the parameter uncertainty analysis when calculating d_{th} for a given aerodynamic diameter (or vice versa). For simplicity, the following assumptions were also assumed: when $d_{\text{th}} > 300$ nm then $\rho_{\text{eff}} = 0.31 \text{ g cm}^{-3}$ and when $d_{\text{th}} < 50$ nm then $\rho_{\text{eff}} = 1.1 \text{ g cm}^{-3}$.

Park *et al* (2003) observed higher effective densities when high sulphur fuel was used as opposed to low sulphur fuel. Olfert *et al* (2007) also observed higher effective densities when the sulphate levels were higher. However, the variation in ρ_{eff} due to different fuel compositions was not considered in this study.

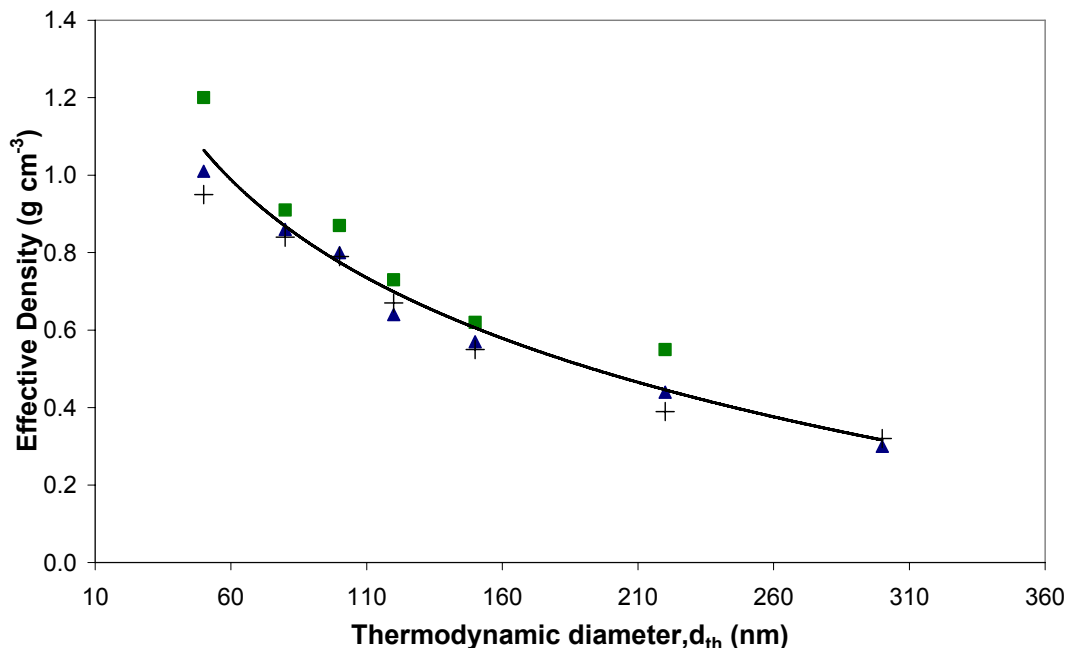


Figure 2 Effective densities of diesel exhaust particles for the John Deere engine running at 10% (■), 50% (+) and 75% (▲) loads determined by Park *et al* (2003). The line shows equation (1), which was fitted to the data.

3.2 Subject related parameters

The parameter probability distributions for the subject related parameters are given in Table 3.

Table 3 Probability distributions for subject related parameters, and representative values.

Description of parameter	Representative value	Probability distribution		
		Form	A	B
Average breathing rate ^a	1.2 m ³ h ⁻¹	Lognormal	1.2 m ³ h ⁻¹	1.3
Fraction breathed through nose (F _n) ^b	1.0	Right-angled triangle 2	0.3	1.0
Slow cleared fraction	0.5	Rectangular	0	0.6
Particle transport rate factor ^c	1.0	Lognormal ^d	1.0	1.7

(a) This distribution has a 95% confidence interval of 0.7 - 2 m³ h⁻¹.

(b) The HRTM assumes a F_n value of 1.0 for a nasal augmenter resting or performing light exercise and a value of 0.3 for a mouth breather performing heavy exercise.

(c) Particle transport rate factor is a factor by which all the particle transport rates are multiplied.

(d) ICRP Publication 66 proposes that the inter-subject variation in any particle transport rate can be represented by a lognormal distribution with a median equal to the reference value and a geometric standard deviation of 1.7.

3.2.1 Breathing rate

The absorbed dose to regions of the lung per WLM is very sensitive to the breathing rate mainly because the intake is directly proportional to the breathing rate (Marsh and Birchall 2000, Birchall and James 1994).

ICRP Publication 66 (ICRP 1994) reported the results of a study to determine the breathing rate of miners performing heavy work in a gold mine in South Africa (South African Chamber of Mines Research Organization 1992). In this study 620 miners wore individual expired air analysers while working, and the oxygen consumption was related to heart frequency. The results indicated that 70% of the miners had a breathing rate greater than 1.2 m³ h⁻¹, and 15% greater than 1.5 m³ h⁻¹. The mean breathing rate was 1.3 m³ h⁻¹. These results are consistent with a lognormal distribution with a geometric mean of 1.29 m³ h⁻¹ and a geometric standard deviation of 1.15. The corresponding 95% confidence interval is 1.0 – 1.7 m³ h⁻¹.

Ruzer *et al* (1995) estimated breathing rates for miners working underground in a metal mine in Tadjikistan. The estimated breathing rates were based on radon progeny exposure measurements and activity chest measurements on about 100 miners. The results for the mean breathing rates (± standard error) were 1.4 ± 0.2 m³ h⁻¹ for drillers, 1.1 ± 0.2 m³ h⁻¹ for assistant drillers and 0.9 ± 0.2 m³ h⁻¹ for personnel working underground. In addition the breathing rates of 14 inspection personnel performing light work were measured directly using the conventional minute volume measurement techniques (Ruzer *et al* 1995). The estimated mean breathing rate was 0.74 ± 0.02 m³ h⁻¹.

The HRTM assumes a mean breathing rate of 1.2 m³ h⁻¹ for a standard worker and 1.7 m³ h⁻¹ for a heavy worker. These values are calculated using the “time-activity-ventilation (TAV) approach that combines:

- the ventilation rates for the four reference levels of physical activity [sleep, sitting, light exercise (LE), and heavy exercise (HE)], and
- the time spent by the worker in each level of physical activity.

Bailey *et al* (1997) considered the TAV approach when estimating uncertainty in the mean breathing rate for children and adults. The authors calculated a range of mean breathing rates by:

- varying the time spent in different levels of activity while holding the ventilation rates constant.
- varying the ventilation rate at each exercise level while holding the time spent in different levels constant.

This approach is repeated here for a miner and the calculated mean breathing rates range from 0.9 to 2.1 m³ h⁻¹ (Tables 4 and 5). The range of times spent in each level of physical activity was based upon a time survey of 6 miners working underground in a metal miner in Tadjikistan (Ruzer *et al* 1995) (Table 4). The range of values for the ventilation rates for each level of physical activity are the values proposed by Bailey *et al* (1997) based on the data of Anderson *et al* (1985), Samet *et al* (1993) and Johnson *et al* (1995) (Table 5). The values for sitting in Table 5 are also consistent with experiment results of Hofmann *et al* (2009). Hofmann *et al* measured the respiratory frequency and the tidal volume in a group of 8 young male adults breathing spontaneously at rest. The corresponding ventilation rates ranged from 0.5 to 1.1 m³ h⁻¹.

Table 4 Range of breathing rates for a miner calculated by varying the time spent in each level of physical activity using the TAV approach.

	Fraction of time ^a		ICRP reference values for ventilation rates, m ³ h ⁻¹ (ICRP 1994)
	Low	High	
Sitting	61%	7%	0.54
LE	38%	76%	1.5
HE	1%	17%	3.0
Mean breathing rate, m ³ h ⁻¹	0.9	1.7	

(a) The estimates for fraction of time spent in each level of physical activity for a miner working underground are based on a time survey of 6 miners (Ruzer *et al* 1995). The low values corresponds to a driller supervisor (bore master, A) and the high values to a driller (shaft sinker, D) (Ruzer *et al* 1995).

Table 5 Range of breathing rates for a miner calculated by varying the ventilation rates for each level of physical activity using the TAV approach.

	Ventilation rate, m ³ h ⁻¹ ^a		Fraction of time for standard worker ^b
	Low	High	
Sitting	0.48	0.90	31%
LE	1.32	2.7	69%
HE			
Mean breathing rate, m ³ h ⁻¹	1.1	2.1	

(a) The lower and higher values for the ventilation rates are given by Bailey *et al* 1997.

(b) The fraction of time spent for each level of physical activity is the HRTM value for a standard worker (ICRP 1994).

A panel of experts from the National Research Council (NRC 1991) recommended a breathing rate of 1.7 m³ h⁻¹ for an underground miner based upon the TAV approach. It is interesting to note that Layton (1993) calculated breathing rates based upon the oxygen requirement to support energy

expenditure by considering daily intakes of food energy from dietary surveys. Layton concluded that there was some evidence that the TAV approach overestimated the breathing rate.

In summary, Table 6 gives breathing rates for miners. Based upon these data, a lognormal distribution with a median of $1.2 \text{ m}^3 \text{ h}^{-1}$ and a geometric standard deviation of 1.3 is assigned to the breathing rates. This gives a 95% confidence interval of $0.7 - 2.0 \text{ m}^3 \text{ h}^{-1}$.

Table 6 Breathing rates for a miner

Reference	Group of workers	Estimated breathing rate, $\text{m}^3 \text{ h}^{-1}$
ICRP Publication 66, p. 198, para. B76 (ICRP 1994)	Gold mine, South Africa	1.3 (1.0 – 1.7) ^a
Ruzer <i>et al</i> (1995)	Metal mine, Tadjikistan:	
	Drillers	1.4 (0.9 – 1.9) ^b
	Assistant drillers	1.1 (0.7 – 1.6) ^b
	Inspection personnel	0.9 (0.5 – 1.3) ^b
	Technical personnel	0.74 (0.74 – 0.78) ^b
ICRP Publication 66 (ICRP 1994)	Standard worker	1.2
	Heavy worker	1.7
NRC (1991)	Mining	1.9
	Haulageway	1.5
Present work ^c	TAV approach:	
	Vary time	0.9 – 1.7
	Vary ventilation rate	1.1 – 2.1

(a) The 95% confidence interval is given in the parentheses.

(b) The 95% confidence interval on the mean is given in the parentheses

(c) Range of breathing rates calculated using the approach adopted by Bailey *et al* (1997). See text for details.

3.2.2 Fraction breathed through nose

The dose to the lung is sensitive to the fraction of the total ventilatory airflow passing through the nose, F_n . Because the nose is a better filter than the mouth, as F_n increases the lung dose decreases (Marsh and Birchall 2000, Birchall and James 1994).

Niinimaa *et al* (1980,1981) studied the breathing patterns of thirty healthy young adults. Twenty of the subjects (“normal augmenters”) switched to oro-nasal breathing at a ventilation rate of about $2.1 \text{ m}^3 \text{ h}^{-1}$ (i.e. between light and heavy exercise). Five subjects continued to breathe through the nose even when exercising vigorously (i.e. “pure nose breathers”). Four subjects were habitual “mouth breathers”, who breathed oro-nasally at all levels of exercise. The remaining subject showed no consistent pattern. Miller *et al* (1988) reviewed these data and based on this review the HRTM assumes the values for F_n given in Table 7.

Table 7 Percentage of total ventilatory airflow passing through the nose, (F_n) in normal nasal augmenters and in mouth breathers (ICRP Publication 66, page 43, Table 11)

Level of exercise	F_n , %	
	Normal nasal augments	Mouth breather
Sleep	100	70
Rest (sitting)	100	70
Light exercise (LE)	100	40
Heavy exercise (HE)	50	30

In order to assign a probability distribution to F_n , the distribution of the breathing modes types was assumed to consist of 20/30 normal nasal augmenters, 4/30 mouth breathers and 5/30 pure nose breathers (Niinimaa *et al* 1980, 1981). Based on the data of Ruzer *et al* (1995), on average a driller spends about 10%, 80% and 10% of their time resting, and performing light and heavy exercise respectively. Taking the F_n values from Table 7, and combining these values with the above breathing mode type distribution and time distribution for a driller, gives the following distribution for F_n (% of time spent in breathing mode in parentheses): $F_n = 0.3$ (1%), $F_n = 0.4$ (11%), $F_n = 0.5$ (7%), $F_n = 1$ (77%). Based on this analysis and for simplicity, a right angle triangular distribution with a minimum at 0.3 and vertex at 1 was assumed for F_n (Table 3).

3.3 Target cell parameters

The parameter probability distributions for the target cell parameters are given in Table 8. It is assumed that both the target cell layer depth and thickness are correlated with the epithelium thickness. Although the epithelium thickness is not used directly in the HRTM, it was used only to introduce a correlation between the target cell layer depth and target cell layer thickness.

Mercer *et al* (1991) measured the airway epithelium thickness and cell depth distribution of surgical specimens of bronchi and bronchioles taken at post mortem from 3 non-smoking adults. The authors states that the variability in airway epithelial thickness for a given airway diameter is relatively small, (~10% for bronchi) whereas the epithelial thickness in different bronchial rings varies as much as 35% from the mean. Based on this work the ICRP adopted a reference value of 55 μm for the epithelial thickness of the BB region of the HRTM. However, the measurement data of Robbins *et al* (1990) and Harley *et al* (1996) indicate a smaller value for the bronchial epithelial thickness. In particular, Harley *et al* (1996) reported a mean depth of the basal cells of 27 μm over airway generations 3 to 6 region whereas the HRTM assumes the basal cells to be uniformly distributed in a 15 μm layer at a depth of 35 μm (i.e. a mean depth of 43 μm) in the BB region, which is consistent with the data of Mercer *et al* (1991).

Based on the data of Mercer *et al* (1991) and Harley *et al* (1996) a rectangular distribution was assumed for the bronchial epithelial thickness with values

ranging from 30 to 75 μm , which reflects intra- and inter-subject variation (Table 8). The lower value is consistent with the data of Harley *et al* (1996). The distribution assumed for the epithelial thickness of the bb region is also based on the data of Mercer *et al* (1991) and also reflects intra- and inter-subject variation (Table 8).

The judgement made in assigning the probability distribution for the mucus sol thickness is based on measurements performed by Gehr reported in ICRP Publication 66, (Tables A.2 to A.4) (ICRP 1994).

Table 8 Probability distributions for target cell related parameters, and HRTM reference values.

Description of parameter	HTRM reference value or representative value	Probability distribution		
		Form	A	B
Bronchial epithelium thickness (E_{BB}) ^a	55 μm	Rectangular	30 μm	75 μm
Bronchial basal cell layer depth ^b	35 μm	$35 E_{BB}/55$		
Bronchial basal cell layer thickness	15 μm	$15 E_{BB}/55$		
Bronchial secretory cell layer depth ^c	10 μm	$10 E_{BB}/55$		
Bronchial secretory cell layer thickness	30 μm	$30 E_{BB}/55$		
Bronchial mucus (gel) thickness	5 μm	Lognormal	4 μm	2
Bronchial mucus (sol) thickness	6 μm	Normal	6 μm	1 μm
Bronchiolar epithelium thickness (E_{bb}) ^a	15 μm	Rectangular	8 μm	22 μm
Bronchiolar secretory cell layer depth ^c	4 μm	$4 E_{bb}/15$		
Bronchiolar secretory cell layer thickness	8 μm	$8 E_{bb}/15$		
Bronchiolar mucus (gel) thickness	2 μm	Lognormal	1.6 μm	2
Bronchiolar mucus (sol) thickness	4 μm	Normal	4 μm	1 μm

- (a) Parameters in bold are not used directly in the model, but are used to introduce correlation between model parameters which are functions of them.
- (b) Depth of basal cell layer is defined here as in ICRP Publication 66 as the distance from the luminal surface of the epithelium (excluding cilia) to the beginning of the basal cell layer.
- (c) Depth of secretory cell layer is defined here as in ICRP Publication 66 as the distance from the luminal surface of the epithelium (excluding cilia) to the beginning of the secretory cell layer.

3.4 Absorption parameters

3.4.1 Unattached radon progeny

Butterweck *et al* (2002) carried out volunteer experiments to determine the absorption rate of unattached radon progeny. Twenty-one volunteers were exposed in a radon chamber with well-controlled aerosol and radon progeny conditions. The aerosol was predominantly unattached radon progeny. Fourteen volunteers inhaled by mouth breathing and 7 volunteers inhaled by nose breathing. Activity measurements were made of radon gas and radon progeny in blood samples taken at the end of a 30 minute exposure. Approximately 7 minutes after exposure, in-vivo measurements of the head were carried out over a 30 minute period. Assuming that the absorption rate is represented by a single rate constant, absorption half-times estimated with the HRTM were 20 to 60 minutes based upon the blood data alone. However, the head measurements showed that the overall clearance half-time was larger than 150 minutes indicating that fast particle transport to the alimentary tract did not occur, at least for the pure mouth breathers. The authors interpreted this as an

indication that a large fraction of the unattached radon progeny is bound to the respiratory tract. To explain the measured activity in the blood it was assumed that a small fraction was rapidly absorbed to blood. Thus, the head and blood data were interpreted with the HRTM by assuming that a small fraction of the unattached progeny is absorbed rapidly to blood while the rest (fraction f_b) is bound to tissue, from which it is absorbed at a rate s_b . The data are consistent with the rapid fraction being between 15% and 30% assuming that the rapid rate is 1000 d^{-1} and s_b is 1.7 d^{-1} (10 h half-time). Thus, the bound fraction, f_b is between 70 and 85%.

Greenhalgh *et al* (1982) observed that the fraction of the ^{212}Pb ions retained in the nasal airways of rats was always greater than that of insoluble particles. The authors interpreted this as evidence in support of uptake of ^{212}Pb ions by the epithelium (i.e. binding occurs). The observed nasal retention and blood data were consistent with the following model: About 60% of the deposited lead being cleared by particle transport and 8% of the deposited lead being rapidly absorbed to blood with a half-time of 15 minutes. The fate of the remaining 32% of the deposited lead was undetermined but the authors suggested that there was some possibility that this lead was bound to the epithelium and cleared to blood with a half-time of 10 h.

Booker *et al* (1969) exposed one volunteer to unattached ^{212}Pb by mouth breathing only. Blood and faecal samples were taken. In-vivo lung counting was carried out to determine lung clearance rates. The lung data indicated a clearance half-time of about 10 h. In contrast to the data of Butterweck *et al* (2002), the blood data indicates that only about 4% was rapidly absorbed to blood assuming a rapid dissolution half-time of 15 minutes and a slow dissolution half-time of 10 h. If only a small percentage of the amount deposited in the ET_2 region is excreted to faeces then this is an indication that most of the unattached ^{212}Pb is bound to the respiratory tract tissue. However, it was reported that about 37% of the amount deposited in the respiratory tract was cleared to faeces in the first 3 days. This is estimated to be about 60% of ET_2 deposit indicating most of the deposit is not bound to the respiratory tract components. Because the results are only for one volunteer firm conclusion cannot be made regarding whether or not binding occurs.

For this study, the probability distributions assigned to the unattached radon progeny absorption parameters are based on the data of Butterweck *et al* (2002) (Table 9).

3.4.2 Attached radon progeny

Marsh and Birchall (1999) re-evaluated published data from volunteer experiments using the HRTM to estimate the absorption rate for lead that is appropriate for short-lived radon progeny (Booker *et al* 1969, Hursh *et al* 1969, Hursh and Mercer 1970). In these experiments volunteers inhaled ^{212}Pb attached to condensation nuclei by mouth breathing only. The blood and lung retention data reported were used in the re-evaluation. Assuming absorption could be represented by a single absorption rate constant the best estimate for

the half-time was 10 h with a 95% confidence interval of ± 2 h. This corresponds to an absorption rate of 1.7 d^{-1} .

As Greenhalgh *et al* (1982) observed a rapid absorption component following intranasal instillation of ionic ^{212}Pb into rats, the volunteer data were re-evaluated again assuming a two component model. The rapid absorption component was assumed to have a half-time of 15 minutes and the rapid dissolution fraction, f_r and the slow dissolution rate, s_s was estimated from the data. The best estimate of f_r was 6% with a 95% confidence interval of $\pm 2\%$. The best estimate of s_s was 1.4 d^{-1} which corresponds to a half-time of 12 h.

Based on the above analysis the probability distributions given in Table 9 were assumed for the absorption parameters of the attached radon progeny.

Table 9 Probability distributions for radon progeny absorption parameters^a, and representative values^{b,c}.

Description of parameter	Representative value	Probability distribution		
		Form	A	B
Unattached, f_r	1.0	Fixed		
Unattached, s_r (d^{-1})	1000	Fixed		
Unattached, f_b	0.8	Rectangular	0.7	0.85
Unattached, s_b (d^{-1}) (10 h half-time)	1.7	Fixed		
Attached, f_r	0.06	Rectangular	0	0.1
Attached, s_r (d^{-1})	67	Fixed		
Attached, s_s (d^{-1}) (12 h half-time)	1.4	Rectangular ^(d)	3.3 (5 h half-time)	1.1 (15 h half-time)
Attached, f_b	0	Fixed		

- (a) The HRTM defines absorption in terms of the following parameters: f_r = rapid dissolution fraction, s_r = rapid dissolution rate, s_s = slow dissolution rate, f_b = bound fraction, s_b = uptake rate from bound state.
 (b) Unattached parameter values are based on results of volunteer experiments performed by Butterweck *et al* 2002.
 (c) Attached parameter values are based on the re-evaluation of published data summarised by Marsh and Birchall, 1999.
 (d) The half-times were varied uniformly between 5 and 15 h.

A question arises as to whether or not a fraction of the attached radon progeny is bound to respiratory tract components. Furthermore, it is unknown if the attached radon progeny that has been deposited in the respiratory tract rapidly separates itself from the aerosol and subsequently has the same absorption characteristics as the unattached progeny. Rapid separation could occur because of alpha recoil and/or physiochemical interactions with the lung fluid. It is noted that the probability that the attached become de-attached from its host due to alpha recoil is about 10% for radon progeny deposited in the lung (Butterweck 2002). These issues are considered in the discussion section (Section 6).

4 CLASSIFICATION OF ERRORS

For epidemiological studies, it is important to distinguish between unshared and shared errors. Shared errors are uncertainties that are 100% correlated between different subjects whereas unshared errors assume no correlation between subjects. If a parameter value is unknown but its true value is assumed to be the same for all subjects then this is a shared error. An example of a shared error would be the uncertainties associated with absorption parameters for the case where subjects inhale the same material; i.e. the HRTM assumes that the absorption rates depend on the material only, even though we do not know the value exactly (ICRP 1994). If the true value is expected to be different for each subject, such as breathing rates, then this is an unshared error. In general, all parameters have a component of both unshared and shared errors, although in some situations one might dominate the other. The dominant type of error assumed for the different types of parameters are given in Table 10. For some parameters, it was difficult to determine which type of error was most appropriate, so these parameters were classified as 'mixed' indicating as having a component of both unshared and shared type errors (Table 10).

Table 10 Type of error assumed for different parameters

Parameter group	Type of error		
	Unshared	Shared	Mixed ^a
Aerosol	Unattached fraction	Attached density ^b	Unattached aerosol size
	Attached aerosol size	Attached shape factor	Unattached dispersion
	Attached dispersion	Attached hygroscopic growth factor	
	Equilibrium factor		
Subject	Breathing rate	Slow cleared fraction	
	Fraction breathed through nose		
	Particle transport rate factor ^c		
Target cell		Epithelium thickness ^d	
		Cilia sol layer thickness	Mucus gel thickness
Absorption		Absorption parameters	

(a) For these parameters it is difficult to determine which type of error dominated and therefore these parameters are classified as having a component of both unshared and shared type errors.

(b) For mines with diesel engines operating, the density of the diesel exhaust particles are assumed to be correlated with the particle size (Section 3.1.2).

(c) Particle transport rate factor is a factor by which all the particle transport rates are multiplied.

(d) Although the epithelium thickness is not used directly in the HRTM, it was used only to introduce a correlation between the target cell layer depth and target cell layer thickness.

The aerosol size distribution of the attached progeny can vary greatly in a mine; indeed measurements show a wide range of aerosol sizes. For, example the measured values of the AMAD are between about 130 nm to 350 nm (Butterweck *et al* 1992). As this variation mainly reflects the actual variation in the true values and not only the measurement error, it can be assumed that

different miners will inhale different aerosol distributions of the attached progeny. Therefore, the attached size distribution can be classified as an unshared error.

To our knowledge there are no published data of the density of aerosol particles attached to radon progeny in a mine atmosphere (Section 3.1). The uncertainty on the density is therefore likely to be dominated by shared errors. For the cases where diesel engines are in operation the diesel aerosol dominates and the density of the diesel aerosol is assumed to be correlated with the size of the particle (Section 3.1.2).

The probability distribution assigned to the depth of the target cells reflects systematic measurement error as well as intra- and inter-subject variation (Table 8). The HRTM assumes a simplified geometric model to represent the location of the target cells within the BB and bb regions (ICRP 1994). Mercer *et al* (1991) noted that the variation in the airway epithelial thickness for a given airway diameter is relatively small, (~10% for bronchi) whereas the epithelial thickness in different bronchial rings varies as much as 35% from the mean. However, the mean depth of the target cells in the BB region reported by Mercer *et al* (1991) and Harley *et al* (1996) differ by about 37%. It is unknown whether this difference arises due to systematic measurement error or due to inter-subject variation. However, because it is a difficult quantity to measure, it is likely that measurement errors dominate the uncertainty. It is also likely that since epithelial thickness (and cell depth) depends on functional requirements of the cells (ICRP 1994, paragraph. 318) it will not be influenced as much by inter-subject variation. Therefore, in this report it assumed that the uncertainty in the depth of the target cells is dominated by shared errors.

The uncertainty in the thickness of the mucous gel overlying the cilia reflects both measurement error and inter-subject variation. Indeed, the thickness of the mucus gel is difficult to determine in histological preparations (National Research Council 1991). Furthermore, for smokers the mucus gel thickness can be greater compared with that from non-smokers. In this report, the uncertainty in the thickness of the mucus gel is classified as 'mixed'; i.e. as having a component of both unshared and shared type errors.

In epidemiological studies, two simplified models of uncertainties have been identified, namely the 'classical' and 'Berkson' models (Schafer and Gilbert 2006). The classical error model generally applies to direct measurements obtained with an imprecise measurement instrument. The additive classical error model for a single source of uncertainty is as follows:

$$\text{Observed value} = \text{true value} + \text{measurement error}$$

Where the *measurement error* is a random variable with a mean of zero and is independent of the true value.

The additive Berkson error model for a single source of uncertainty is as follows:

$$\text{True value} = \text{observed value} + \text{individual peculiarity}$$

Where the *individual peculiarity* is a random variable with a mean of zero and is independent of the observed value.

The errors associated with internal dosimetry can be considered as Berkson type errors (Schafer and Gilbert 2006). The *individual peculiarities* represent the inability of the dosimetric model to predict the individual's true dose for a given exposure. The *observed value* represents the calculated value.

5 RESULTS

5.1 Exposure conditions: Wet drilling + medium ventilation

The frequency distributions of the lung regional absorbed doses per WLM are given in Figures 3 and 4, and the parameter values characterising the distribution are given in Table 11. These calculations were performed using the parameter probability distributions given in Tables 1, 3, 8 and 9 assuming wet drilling + medium ventilation (and no diesel engines) for the exposure conditions. The frequency distribution of the lung regional absorbed doses per WLM can be approximated by a lognormal distribution (Figures 3 and 4).

Table 11 Parameters characterising the distribution of absorbed doses to regions of the lung for a miner. Exposure conditions assumed: Wet drilling + medium ventilation.

Region ^a	Arithmetic mean, (mGy WLM ⁻¹)	Coefficient of variation ^b	Geometric mean, (mGy WLM ⁻¹)	σ_g ^c
BB _{bas}	6.7	54%	5.9	1.6
BB _{sec}	13.6	61%	11.7	1.7
bb	8.4	32%	8.0	1.4
AI	0.44	31%	0.42	1.3

a) BB_{bas} = bronchial basal cells; BB_{sec} = bronchial secretory cells; bb = bronchiolar; AI = Alveolar interstitial.

b) Coefficient of variation is the ratio of the standard deviation to the arithmetic mean

c) σ_g = geometric standard deviation.

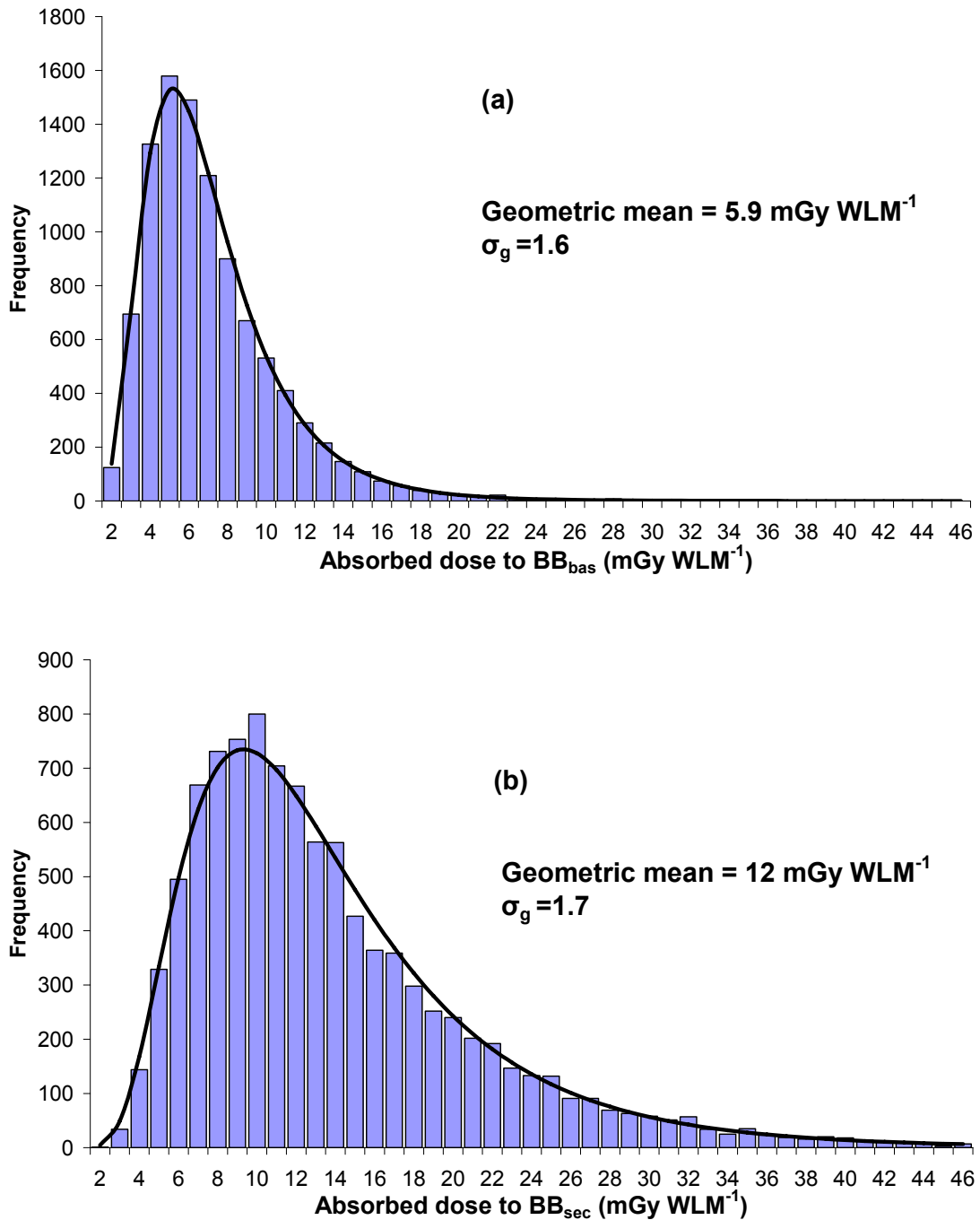


Figure 3 Frequency distribution of the absorbed dose to (a) BB_{bas} and to (b) BB_{sec}. The line shows a theoretical lognormal distribution with values of a geometric mean and a σ_g given on the figure. Exposure conditions: Wet drilling + medium ventilation.

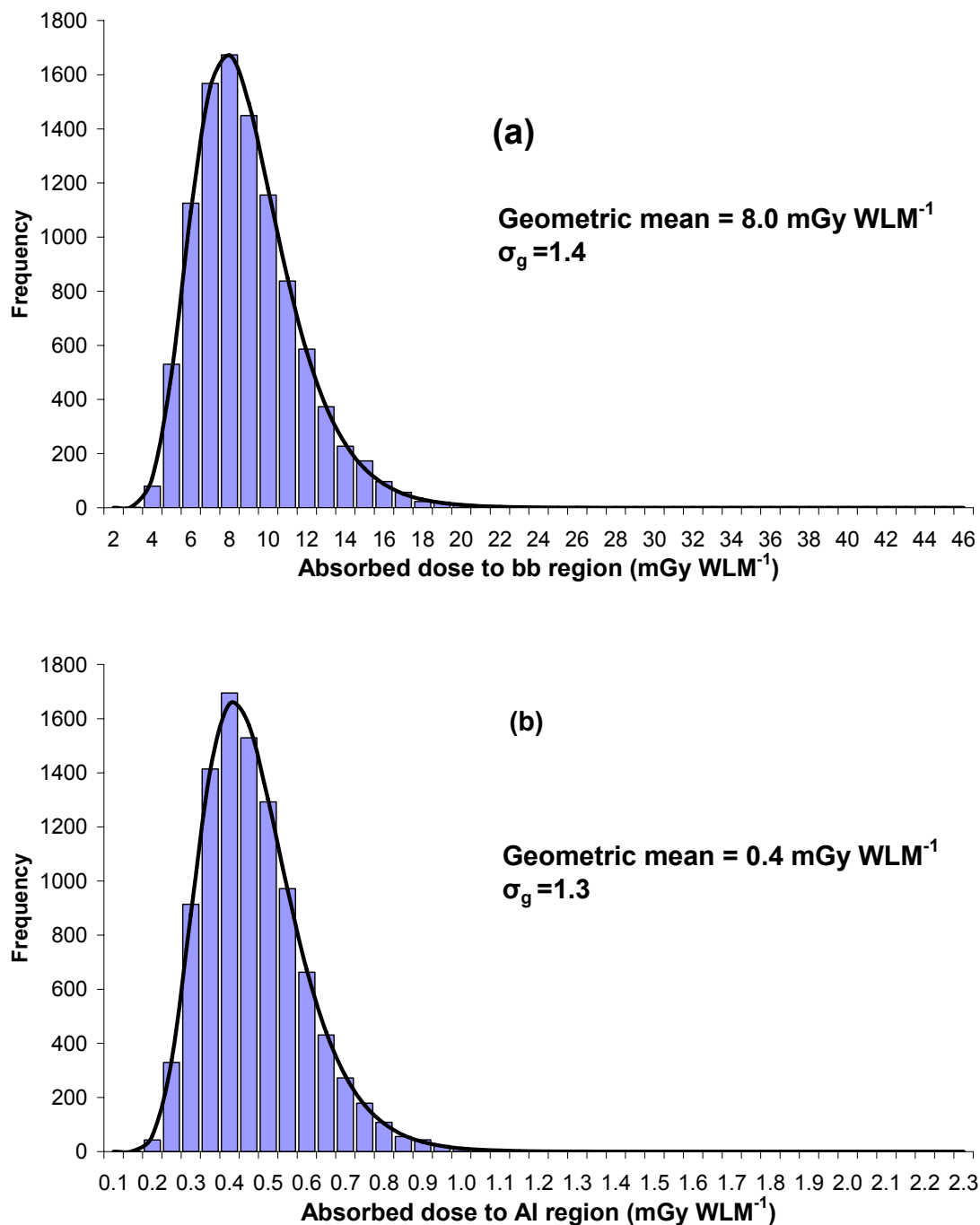


Figure 4 Frequency distribution of the absorbed dose to (a) bb and to (b) AI regions of the lung. The line shows a theoretical lognormal distribution with values of a geometric mean and a σ_g given on the figure. Exposure conditions: Wet drilling + medium ventilation.

Table 12 gives the lung regional absorbed doses per WLM obtained using the representative values given in Tables 1, 3, 8 and 9. These absorbed doses are lower than the arithmetic and geometric means of the corresponding frequency distributions. This is because the model is non-linear and because for a few

parameters the representative value is not equal to the mean value of the parameter distribution.

Table 12 Lung regional absorbed doses assuming representative values for a mine conditions^a. Exposure conditions assumed: Wet drilling + medium ventilation.

Region or target tissue	Absorbed doses per WLM (mGy WLM ⁻¹)
Bronchial basal cells, BB _{bas}	4.5
Bronchial secretory cells, BB _{sec}	8.7
Bronchiolar, bb	6.8
Alveolar interstitial, AI	0.36

(a) Representative values given in Tables 1, 3, 8 and 9.

Frequency distributions of lung regional absorbed doses per WLM have also been calculated by varying certain groups of parameters:

- aerosol parameters of Table 1
- subject related parameters of Table 3
- target cell parameters of Table 8
- absorption parameters of Table 9
- parameters classified as mainly comprising of unshared errors (Table 10)
- parameters classified as mainly comprising of shared errors (Table 10)
- parameters classified as 'mixed' (i.e. as having a component of both unshared and shared type errors, Table 10).

The results are summarised in Table 13 and the contributions to the overall uncertainty of the dose due to the uncertainties of each group of parameters can be seen.

Table 13 Parameters characterising the distribution of absorbed doses to regions of the lung for a miner obtained by varying different parameter values. Exposure conditions assumed: Wet drilling + medium ventilation. (GM= geometric mean in units of mGy WLM⁻¹, σ_g = geometric standard deviation.)

Parameters varied	Absorbed doses , mGy WLM ⁻¹							
	BB _{bas}		BB _{sec}		bb		AI	
	GM	σ_g	GM	σ_g	GM	σ_g	GM	σ_g
Aerosol	5.1	1.3	10.0	1.2	7.9	1.3	0.41	1.2
Subject	5.0	1.3	9.5	1.3	6.9	1.2	0.37	1.3
Cell	4.6	1.3	9.0	1.4	6.8	1.1	-	-
Absorption	4.4	1.03	8.6	1.03	6.7	1.03	0.36	1.03
All	5.9	1.6	11.7	1.7	8.0	1.4	0.42	1.3
Unshared	5.7	1.5	11.1	1.5	7.8	1.3	0.40	1.3
Shared	4.7	1.3	9.1	1.4	7.0	1.2	0.37	1.1
Mixed	4.5	1.07	8.7	1.07	6.8	1.02	0.36	< 1.01

5.2 Exposure conditions: Wet drilling + good ventilation + diesel engines

The parameter values characterising the frequency distributions of the lung regional absorbed doses per WLM distribution are given in Table 14. These calculations were performed using the parameters probability distributions given in Tables 2, 3, 8 and 9 assuming 'wet drilling + good ventilation + diesel engines'. These frequency distributions of the lung regional absorbed doses per WLM can be approximated by a lognormal distribution.

Table 14 Parameters characterising the distribution of absorbed doses to regions of the lung for a miner. Exposure conditions assumed: Wet drilling + good ventilation + diesel engines.

Region ^a	Arithmetic mean, (mGy WLM ⁻¹)	Coefficient of variation ^b	Geometric mean, (mGy WLM ⁻¹)	σ_g ^c
BB _{bas}	4.3	49%	3.9	1.6
BB _{sec}	8.7	55%	7.7	1.7
Bb	6.9	35%	6.6	1.4
AI	0.35	35%	0.33	1.4

(a) BB_{bas} = bronchial basal cells; BB_{sec} = bronchial secretory cells; bb = bronchiolar; AI = Alveolar interstitial.

(b) Coefficient of variation is the ratio of the standard deviation to the arithmetic mean

(c) σ_g = geometric standard deviation.

The arithmetic means in Table 14 for exposure conditions 'wet drilling + good ventilation + diesel engines' are lower than those of Table 11 for the exposure conditions 'wet drilling + medium ventilation'. However, the percentage differences between the corresponding arithmetic means (of Tables 11 and 14) are smaller compared with coefficient of variation. The corresponding geometric standard deviations are similar for both exposure conditions (compare Tables 11 & 14).

Table 15 gives the lung regional absorbed doses per WLM obtained using the representative values given in Tables 2, 3, 8 and 9. These absorbed doses are lower than the arithmetic and geometric means of the corresponding frequency distributions given in Table 14.

Table 15 Lung regional absorbed doses assuming representative values for a mine conditions^a. Exposure conditions assumed: Wet drilling + good ventilation + diesel engines.

Region or target tissue	Absorbed doses per WLM (mGy WLM ⁻¹)
Bronchial basal cells, BB _{bas}	3.1
Bronchial secretory cells, BB _{sec}	6.1
Bronchiolar, bb	6.5
Alveolar interstitial, AI	0.31

(a) Representative values given in Tables 2, 3, 8 and 9.

Frequency distributions of lung regional absorbed doses per WLM have also been calculated by varying certain groups of parameters: aerosol parameters of Table 2; subject related parameters of Table 3; target cell parameters of Table 8; absorption parameters of Table 9; and parameters that are classified as unshared, shared or mixed (Table 10). The results are summarised in Table 16 and the contributions to the overall uncertainty of the dose due to the uncertainties of each group of parameters can be seen.

Table 16 Parameters characterising the distribution of absorbed doses to regions of the lung for a miner obtained by varying different parameter values. Exposure conditions assumed: Wet drilling + good ventilation + diesel engines. (GM= geometric mean in units of mGy WLM⁻¹, σ_g = geometric standard deviation.)

Parameters varied	Absorbed doses , mGy WLM ⁻¹							
	BB _{bas}		BB _{sec}		bb		AI	
	GM	σ_g	GM	σ_g	GM	σ_g	GM	σ_g
Aerosol	3.5	1.3	6.9	1.3	6.6	1.3	0.33	1.3
Subject	3.3	1.2	6.4	1.2	6.4	1.2	0.31	1.3
Cell	3.1	1.3	6.3	1.4	6.4	1.1	-	-
Absorption	3.0	1.03	6.0	1.03	6.4	1.03	0.31	1.03
All	3.9	1.6	7.7	1.7	6.6	1.4	0.33	1.4
Unshared	3.8	1.4	7.5	1.4	6.7	1.4	0.34	1.4
Shared	3.1	1.3	6.2	1.4	6.3	1.1	0.31	1.03
Mixed	3.1	1.07	6.1	1.08	6.5	1.02	0.31	< 1.01

6 DISCUSSION

Based upon the data of Butterweck *et al* (2002) it was assumed that the unattached radon progeny binds to the respiratory tract. However, the data of Booker *et al* (1969) indicates that most of the unattached fraction is not bound to the respiratory tract (Section 3.4.1). For the attached radon progeny, it was assumed that no binding occurs (Table 9). The uncertainty parameter analysis did not take account of the uncertainty in whether or not the attached progeny binds to the respiratory tract. If binding does occur then the doses will be greater as the assumption is made that retained activity is physically closer to the target cells. This uncertainty can be considered as a systematic error on the dose.

Table 17 gives the regional absorbed doses to the lung assuming either the radon progeny are (i) not bound to lung tissue or (ii) a fraction is bound to lung tissue. The absorption parameter values assumed are given in Table 18. The % differences in the doses are < 10% for the BB_{sec}, bb and AI regions whereas for the BB_{bas} it is about 80% (Table 17).

If binding does occur then the absorbed dose to BB_{bas} can increase by up to about 63% compared with the absorbed dose of 4.5 mGy WLM^{-1} (Table 12) calculated with the representative values given in Tables 1, 3, 8 and 9.

Table 17 Comparison of lung regional absorbed doses assuming either the radon progeny are (i) not bound to lung tissue or (ii) a fraction is bound to lung tissue. Exposure conditions assumed: Wet drilling + medium ventilation.

Region ^a	Absorbed doses , mGy WLM^{-1}		% difference
	No binding ^b	Binding occurs ^b	
BB_{bas}	4.1	7.3	80%
BB_{sec}	8.7	9.2	6%
bb	6.8	7.3	8%
AI	0.36	0.36	1%

(a) BB_{bas} = bronchial basal cells; BB_{sec} = bronchial secretory cells; bb = bronchiolar; AI = Alveolar interstitial.

(b) Representative values for absorption parameter values are given in Table 18. Other parameter values are given in Tables 1, 3 and 8.

Table 18 Representative values for radon progeny absorption parameters^a assuming either the radon progeny are (i) not bound to lung tissue or (ii) a fraction is bound to lung tissue. Exposure conditions assumed: Wet drilling + medium ventilation.

Description of parameter ^a	Representative value	
	No binding ^b	Binding occurs
Unattached, f_r	0.04	1.0
Unattached, s_r (d^{-1})	67 (15 min half-time)	1000
Unattached, s_s (d^{-1})	1.7 (10 h half-time)	
Unattached, f_b	0	0.8
Unattached, s_b (d^{-1})	-	1.7 (10 h half-time)
Attached, f_r	0.06	1
Attached, s_r (d^{-1})	67 (15 min half-time)	67
Attached, s_s (d^{-1})	1.4 (12 h half-time)	-
Attached, f_b	0	0.94
Attached, s_b (d^{-1})	-	1.4 (12 h half-time)

(a) The HRTM defines absorption in terms of the following parameters: f_r = rapid dissolution fraction, s_r = rapid dissolution rate, s_s = slow dissolution rate, f_b = bound fraction, s_b = uptake rate from bound state.

(b) Assuming no binding, the unattached parameter values are based upon the data of Booker *et al*, 1969 and the attached parameter values are based on the re-evaluation of published data summarised by Marsh and Birchall, 1999.

(c) Assuming binding occurs, the unattached parameter values are based on results of volunteer experiments performed by Butterweck *et al* 2002.

Another source of systematic error that has not been considered is the uncertainty in the model structure. For comparison purposes, Winkler-Heil *et al* (2007) calculated the absorbed doses to the BB and bb regions arising from inhalation of radon progeny using the IDEAL model, which is a stochastic airway generation model that consists of a variable number of asymmetric airway generations (12 to 20). Values of absorbed dose to the BB and bb regions were approximately 10% and 40% lower than that calculated with the HRTM respectively. The authors noted that one of the important issues affecting the comparison is the averaging procedure for the cellular doses used in IDEAL. The authors used an averaging procedure based on equal weight but noted

that weighting by the number of cells in a given generation may be more relevant from a radiological point of view.

After modifying the IDEAL model, Winkler-Heil (2008) repeated her calculations with IDEAL assuming model parameter values given in Winkler-Heil *et al* (2007). Values of absorbed dose to the BB_{bas}, BB_{sec} and bb regions were approximately 30%, 30% and 40% lower than that calculated with the HRTM respectively.

The inter-subject variability in the deposition efficiencies of the HRTM was not considered. However, the variation in deposition caused by the uncertainty in the aerosol parameter values and breathing rates was considered. This additional source of uncertainty will be considered in future studies.

7 CONCLUSION

A parameter uncertainty analysis has been carried out with the HRTM to derive the frequency distribution of the absorbed doses to regions of the lung per unit exposure to radon progeny. Two exposure scenarios were considered: (i) wet drilling + medium ventilation (with no diesel aerosol), and (ii) wet drilling + good ventilation + diesel engines. The distributions of the absorbed doses were approximately lognormal and the parameter values characterising these distributions are given in Tables 11 and 14.

For the exposure scenario of wet drilling + medium ventilation (with no diesel aerosol), the distribution of absorbed doses to BB_{bas} has a geometric mean (GM) of 5.9 mGy WLM⁻¹ and a geometric standard deviation (σ_g) of 1.6. The corresponding values for the 'wet drilling + good ventilation + diesel engines' exposure scenario are: GM = 3.9 mGy WLM⁻¹ and σ_g = 1.6. The GM is lower but the σ_g value is similar.

The uncertainties for different parameters were classified as one of the following: shared, unshared and mixed (Section 4). The uncertainties on the absorbed doses arising from shared, unshared or mixed errors were determined (Tables 13 and 16). The unshared errors contributed the most to the overall uncertainty.

In addition, to the above uncertainties, the systemic error caused by the uncertainty in whether or not radon progeny binds to the respiratory tract was estimated. If binding does occur then the absorbed dose to the BB_{bas} can increase up to about 63%. However, in comparison binding makes little difference to the absorbed doses to BB_{sec} or bb (< 10%).

8 ACKNOWLEDGEMENTS

The authors would like to thank Dr G Butterweck and Dr J Porstendörfer for advice on aerosol parameter values based on their measurement data. The authors would also like to thank D Laurier, B Grosche, M Kreisheimer, M

Möhner, M Tirmarche and L Tomasek for their contribution in this work with regard to the miner data, the classification of miners and for interesting discussions with regard to the classification of errors. The authors would also like to thank W Hofmann, E Blanchardon and D Nosske for reviewing this work and for interesting discussions. This work was partially supported by the European contract Alpha-Risk (FP6-516483).

9 REFERENCES

- Anderson E, Braune N, Duletsky S, Ramig J and Warri T (1985). Development of Statistical Distributions of Ranges of Standard Factors in Exposure Assessments. EPA 600/8.85/010 Environmental Protection Agency, Washington DC.
- Bailey MR, Harrison JD, Jones KA, Marsh JW and Prosser SL (1997). Uncertainties in aspects of internal dosimetry relevant to accident consequence assessment codes. Chilton, NRPB-M763.
- Bigu J (1990). Electrical charge characteristics of long-lived radioactive dust. *Health Phys* **58**(3), 341-350.
- Birchall A and James AC (1994). Uncertainty analysis of the effective dose per unit exposure from radon progeny and implications for ICRP risk-weighting factors. *Radiat Prot Dosim* **53**(1-4), 133-140.
- Booker DV, Chamberlain AC, Newton D and Stott ANB (1969). Uptake of radioactive lead following inhalation and injection. *Br J Radiol* **42**, 457-466.
- Butterweck G (2002). Paul Scherrer Institut (PSI), CH-5232 Villigen PSI, Switzerland. Private communication.
- Butterweck G, Porstendörfer J, Reineking A and Kesten J (1992). Unattached fraction and the aerosol size distribution of the radon progeny in a natural cave and mine atmospheres. *Radiat Prot Dosim* **45**(1-4), 167-170.
- Butterweck G, Schuler Ch, Vezzù G, Müller R, Marsh JW, Thrift S and Birchall A (2002). Experimental determination of the absorption rate of unattached radon progeny from respiratory tract to blood. *Radiat Prot Dosim* **102**(4), 343-348.
- Cavallo A (2000). The radon equilibrium factor and comparative dosimetry in homes and mines. *Radiat Prot Dosim*, **92**(4) 295-298.
- Greenhalgh JR, Birchall A, James AC, Smith H and Hodgson A (1982). *Differential retention of ²¹²Pb ions and insoluble particles in nasal mucosa of the rat.* *Phys Med Biol* **27**, 837-851.
- Harley N (2007). Private communication, New York University School of Medicine, 550 First Avenue, New York, 10016, USA.
- Harley NH, Cohen BS and Robbins ES (1996). The variability in radon decay product bronchial dose. *Environ Int* **22** (Suppl. 1): S959-S964.
- Hofmann W, Morawska L, Winkler-Heil R and Moustafa M (in press). Deposition of combustion aerosols in the human respiratory tract: Comparison of theoretical predictions with experimental data considering nonspherical shape. *Inhalation Toxicology*.
- Hursh JB and Mercer TT (1970). Measurement of ²¹²Pb loss rate from human lungs. *J Appl Physiol* **28**, 268-274.
- Hursh JB, Schraub A, Sattler EL and Hofmann HP (1969). Fate of ²¹²Pb inhaled by human subjects. *Health Phys* **16**, 257-267.
- ICRP (1990). 1990 Recommendations of the International Commission on Radiological Protection. ICRP Publication 60. *Ann ICRP* **21**(1-3), Oxford, Pergamon Press.

- ICRP (1994). Human respiratory tract model for radiological protection. ICRP Publication 66. *Ann ICRP* **24**(1-3), Oxford, Pergamon Press.
- Iman RL and Conover WJ (1982). Sensitivity analysis techniques: Self teaching curriculum. NUREG/CR-2350, SAND81-1978, Sandia National Laboratories, Albuquerque NM.
- Johnson T, Capel J, McCoy M and Mozier JW (1995). Estimation of ozone exposures experienced by outdoor workers in nine urban areas using a probabilistic version of NEM. Contract No. 63-D-30094, report JTN 453207-1. US Environmental Protection Agency, Office of Air Quality and Standards, Research Triangle Park, North Carolina 27711, USA.
- Layton DW (1993). Metabolically consistent breathing rates for use in dose assessments. *Health Phys* **64**, 23-26.
- Marsh JW and Birchall A (1999). Determination of lung-to-blood absorption rates for lead and bismuth that are appropriate for radon progeny. *Radiat Prot Dosim* **83**(4), 331-337.
- Marsh JW and Birchall A (2000). Sensitivity analysis of the weighted equivalent lung dose per unit exposure from radon progeny. *Radiat Prot Dosim*, **87**(3) 167-178.
- Marsh JW, Bessa Y, Birchall A, Blanchardon E, Hofmann W, Nosske D and Tomasek L (2008). Dosimetric models used in the Alpha-Risk project to quantify exposure of uranium miners to radon gas and its progeny. *Radiat Prot Dosim*, **103**(1) 101-106.
- Mercer RR, Russell ML and Crapo JD (1991). Radon dosimetry based on the depth distribution of nuclei in human and rat lungs. *Health Phys* **61** 117-130.
- National Research Council (1991). Comparative dosimetry of radon in mines and homes. National Academy Press, Washington DC. ISBN 0-309-04484-7.
- Niinimaa V, Cole P, Mintz S and Shephard RJ (1980). The switching point from nasal to oronasal breathing. *Respir Physiol* **42**, 61-71.
- Niinimaa V, Cole P, Mintz S and Shephard RJ (1981). Oronasal distribution of respiratory airflow. *Respir Physiol* **43**, 69-75.
- Olfert JS, Olfert Symonds JPR and Collings N (2007). The effective density and fractal dimensions of particles emitted from a light-duty vehicle with a diesel oxidation catalyst. *Aerosol Sci* **38** 69-82.
- Park K, Cao F, Kittelson DB and McMurry PH (2003). Relationship between particle mass and mobility for diesel exhaust particles. *Environ Sci Technol* **37**, 577-583.
- Porstendörfer J (2001). Physical parameters and dose factors of the radon and thoron decay products. *Radiat Prot Dosim*, **94**(4), 365-373.
- Porstendörfer J and Reineking A (1999). Radon: characteristics in air and dose conversion factors. *Health Phys* **76**(3), 300-305.
- Robbins ES, Meters OA and Harley NH (1990). Quantification of the nuclei of human bronchial epithelial cells from electron micrographs for radon risk analysis. In: Proceedings of XIIth International Congress for Electron Microscopy (San Francisco, CA: San Francisco Press).
- Ruzer LS, Nero AV and Harley NH (1995). Assessment of lung deposition and breathing rate of underground miners in Tadzhikistan. *Radiat Prot Dosim* **58**, 261-268.
- Samet JM, Lambert WE, James DS, Mermier CM and Chick TW (1993). Assessment of heart rate as a predictor of ventilation. In: *Noninvasive methods for measuring ventilation in mobile subjects, Research Report Number 59*. Health Effects Institute, Cambridge MA, USA, pp 19-69.
- Schafer DW and Gilbert ES (2006). Some statistical implications of dose uncertainty in radiation dose – response analyses. *Radiat Res* **166**, 303-312.
- Sinclair D, Countess RJ and Hoopes GS (1974). Effect of relative humidity on the size of atmospheric aerosols particles. *Atmos Environ*, **8**, 1111-1117.
- South African Chamber of Mines Research Organization (1992). Underground Environment. Preliminary report on ventilation rate of mine workers. DG. Wymer and A Vander Linde, personal communication.

- Weingartner E, Burtscher H and Baltensperger U (1997). Hygroscopic Properties of carbon and diesel soot particles. *Atmospheric Environ* **31** 2311-2327.
- Winkler-Heil R (2008). Private communication. University of Salzburg, Hellbrunner Str. 34, 5020 Salzburg, Austria.
- Winkler-Heil R, Hofmann W, Marsh JW and Birchall A (2007). Comparison of radon lung dosimetry models for the estimation of dose uncertainties. *Radiat Prot Dosim* **127**, 1-4.